J. Astrophys. Astr. (2006) **27,** 37–45

Luminosity Dependent Study of the High Mass X-ray Binary Pulsar 4U 0114 + 65 with ASCA

U. Mukherjee & B. Paul
Tata Institute of Fundamental Research, Homi Bhabha Road, Colaba, Mumbai 400 005, India.

Received 2005 October 29; accepted 2006 February 21

Abstract. Here we report the spectral characteristics of the high and low states of the pulsar 4U 0114 + 65 and examine the change in the parameters of the spectral model. A power law and a photoelectric absorption by material along the line of sight together with a high energy cut-off suffice to describe the continuum spectrum in both the states. A fluorescence iron line at ∼6.4 keV is present in the high as well as in the low state, though it is less intense in the latter. The photon index, cut-off energy and e-folding energy values hardly show any discernible change over the states. We compare these spectral characteristics as observed with ASCA with those of other satellites. We also compare the spectral characteristics of 4U 0114 + 650 with other X-ray sources which show intensity variation at different time scales.

Key words. Stars: pulsar: individual (4U 0114 + 65)—X-rays: pulsar.

1. Introduction

4U 0114 + 650 is a pulsar which belongs to the class of High Mass X-ray Binaries (HMXB). It was discovered in the SAS-3 Galactic Survey (Dower & Kelley 1977). The pulsar has a B1Ia supergiant optical companion and the binary system is at a distance of ∼7 kpc (Reig *et al.* 1996). Crampton *et al.* (1985) reported an orbital period of ∼11.59 days for this HMXB from the optical radial velocity measurements. Their measurements were not able to distinguish between a circular or elliptical orbit for this binary. Corbet *et al.* (1999) obtained X-ray intensity modulations at a period of ∼11.63 days from the long term light curve of RXTE-ASM. In addition to the orbital modulation, the X-ray light curve of this source shows considerable variability, with flaring activity for a few hours (Apparao *et al.* 1991; Finley *et al.* 1992) and also short-term flickering for minutes (Koenigsberger *et al.* 1983). The presence of a ∼2.8 hr periodicity has been observed in the X-ray light curves of 4U 0114 + 65 from the analysis of archival EXOSAT and ROSAT data (Finley *et al.* 1992). This has been re-confirmed by Corbet *et al.* (1999) with the data from RXTE-ASM and Hall *et al.* (2000) with RXTE-PCA. This periodicity has been interpreted as the spin period of the pulsar. Very recently, Farrell *et al.* (2005) reported the detection of a superorbital period of ∼30.7 days in this pulsar by analyzing the data of RXTE-ASM.

The X-ray spectrum emanating from the pulsar is nicely fitted with a generic model applicable in the case of HMXBs consisting of a power law with an absorption along

the line of sight, modified at high energies by an exponential cut-off. There is also the presence of a fluorescent line at $\sim$6.4 keV due to neutral or lowly ionized iron (Yamauchi *et al.* 1990; Masetti *et al.* 2005). The typical values of the model parameters are a photon index $\sim$1, the cut-off energy at $\sim$8 keV and the e-folding energy at $\sim$20 keV. The column density values vary from $\sim 3 \times 10^{22}$ atoms cm^{-2} (Hall *et al.* 2000, with RXTE) to $\sim 15 \times 10^{22}$ atoms cm^{-2} (Masetti *et al.* 2005, with BeppoSAX). X-ray spectroscopy of this source during the different intensity states has been carried out in different energy bands with data from various satellites. Like, Koenigsberger *et al.* (1983) with combined data from Einstein Observatory, HEAO-1 and OSO-8, Yamauchi *et al.* (1990) with GINGA, Apparao *et al.* (1991) with EXOSAT, Hall *et al.* (2000) with RXTE, Bonning & Falanga (2005) with INTEGRAL and Masetti *et al.* (2005) with BeppoSAX.

A very preliminary overall X-ray spectral analysis of this source observed by ASCA was reported earlier (Ebisawa 1997). The preliminary analysis showed the presence of a fluorescent iron-line at $\sim$6.4 keV and reported a variable hydrogen column density (N_H). But the broad-band spectral characteristics of 4U 0114 + 65 has now been established with BeppoSAX which confirms the presence of a high energy cut-off in the spectra in both the states. Since the cut-off energy falls within the ASCA energy band, we have reanalyzed the ASCA data and determined the column density and iron-line parameters accurately. Since ASCA has a better spectral resolution compared to other detectors which have observed this source and it also has a low energy coverage comparable to BeppoSAX, it is imperative to investigate the source in detail with ASCA. In this paper, we map the spectral change of 4U 0114 + 650 with ASCA at two different intensity levels. We also compare the spectral characteristics of this HMXB with the results obtained from other satellites at different orbital phases. For this purpose, we have described the observations in section 2, the data analysis and results in section 3 and thereafter discuss our results in the last section.

2. Observations

The present observation of the pulsar 4U 0114 + 65 was carried out by ASCA on 1997-02-10 (at an orbital phase of 0.19) for a useful exposure time of $\sim$25 ks. The time span between the start and the end of the observation was $\sim$55 ks, which is about 5.5% of the orbital period. ASCA has two gas-imaging spectrometers (GIS) and two solid-state imaging spectrometers (SIS). The energy resolutions are 500 eV and 130 eV (FWHM) @ 6 keV for the GIS and SIS detectors respectively. For more details about ASCA, the reader is referred to Tanaka *et al.* (1994). During this observation, the GIS was operated in the standard PH mode and the SIS was used in the Bright mode.

3. Data reduction, analysis and results

For this work, we have used the standard data reduction procedure of the ASCA guest observer facility. We have taken the archival screened data for our analyses. The source light curves and the spectra were obtained from circular regions of radii of 6′ and 3′ around the centroid of the source from the GIS and SIS respectively. The background

light curves and spectra were extracted from the source-free part of the field-of-view from similar circular regions. For better statistics, the light curves and spectra from the GIS2 and GIS3 detectors, as well as the data from the SIS0 and SIS1 detectors were combined together. A detailed description of ASCA data reduction and analysis can be found in http://heasarc.gsfc.nasa.gov/docs/asca/abc/abc.html

3.1 *The light curve*

We have shown the total GIS and SIS background subtracted light curves with a binsize of ~ 100 s in Fig. 1. The light curve shows flaring state during the first 20 ks and low state afterwards. On the average, there is a decay of the count rate from 10 ks onwards as can be seen from the light curves. The intensity at the peak of the flare is ~ 12–15 times than the persistent low level emission. At times, the intensity almost drops down to zero (at ~ 22 and ~ 32 ks in Fig. 1). In addition, there are short time-scale intensity variations for a few minutes. For our analyses, we have divided the whole light curve into two sections. The first section corresponds to the high state and is between 0 and 18 ks. The other half is ascribed to the low state of the source. The GIS and SIS average count rates (background subtracted) for the whole observation are 3.9 and 3.0 count s^{-1} respectively. The background subtracted count rates for the high state GIS and SIS light curves are 7.8 and 6.5 count s^{-1} respectively, whereas the low state count rates for the said instruments are 2.0 and 1.7 count s^{-1}. We were not able to detect the ~ 2.7 hr periodicity from the light curves. Strong aperiodic variability at short and long time scales and inadequate exposure prohibits us from finding pulsations at the reported 2.7 hr spin period.

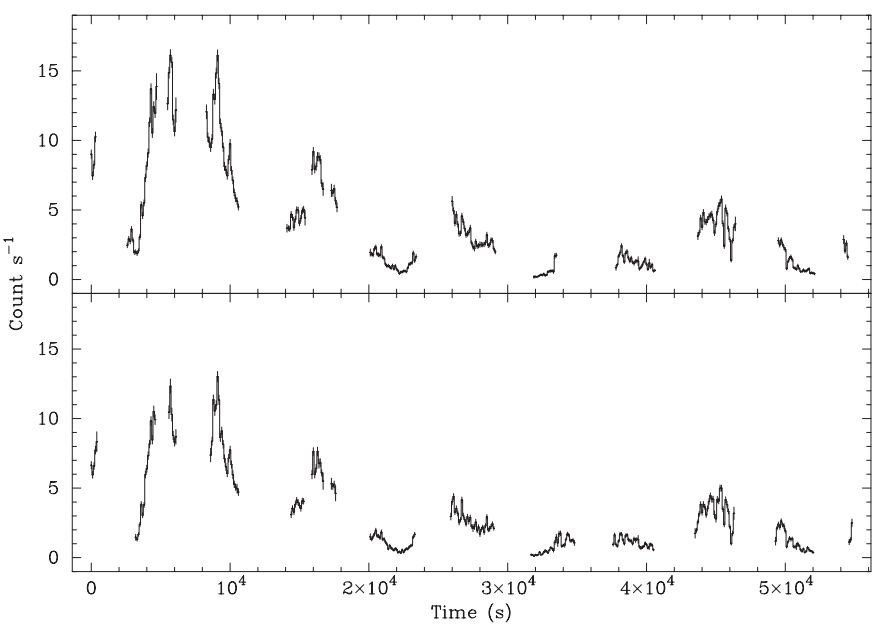

Figure 1. The background subtracted light curves of 4U 0114 + 65 taken on 1997-02-10 with detectors onboard the ASCA Observatory are shown here with binsize of 100 s. The top panel shows the GIS light curve in the 0.7–10.0 keV band and the bottom panel shows the SIS light curve in the 0.5–9.0 keV band.

3.2 *The spectral model and the fitting*

The spectral fitting was carried out in XSPEC version 11.2.0 (Shafer *et al.* 1989). After appropriate background subtraction, the GIS and SIS spectra were fitted simultaneously. The energy bands used for the fitting was 0.7–10.0 keV for the GIS and 0.5–9.0 keV for the SIS, where the effective areas and energy responses of the detectors are well defined. The 1024 channels of the GIS and the 512 channels of the SIS spectra were grouped suitably. In all of our fits described below, we have included an interstellar photoelectric absorption along the line of sight (*wabs* in XSPEC). A constant factor was incorporated to account for the relative normalization of the GIS and SIS detectors.

We extracted the spectra for the high and the low intensity levels (as defined above) respectively. The high state spectrum was first fitted with a simple power law and residuals were seen between $\sim$6.2 and 6.6 keV. This prompted us to include a Gaussian line in the model. And that expectedly improved the fit from a χ^2 of 417 for 265 degrees of freedom to a χ^2 of 318 for 262 degrees of freedom. Though the reduced χ^2 of 1.2 was reasonably acceptable, there apparently remained some residuals between 1.0 and 3.0 keV. Also from $\sim$7 keV onwards there was a hint of a high energy cut-off in the residuals. Hence we added the high energy cut-off in our model. That helped to weed out the above mentioned features in the residuals altogether. Figure 2 shows the high state spectrum along with the residuals. The low state spectra was fitted likewise and we obtained an acceptable fit without any feature in the residuals. The low state spectrum is shown in Fig. 3 with the best fit model and the residuals.

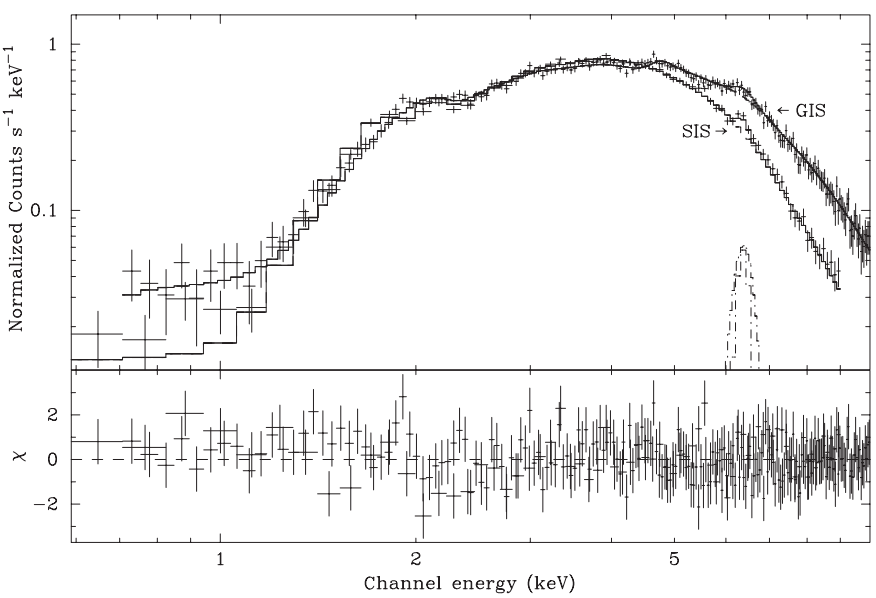

Figure 2. The high intensity level X-ray spectrum of 4U 0114 + 65 measured with the ASCA SIS and GIS are shown in the top panel along with the best fitted spectral model components as histograms. Contribution of each data point in the spectrum to the total χ^2 is shown in the bottom panel.

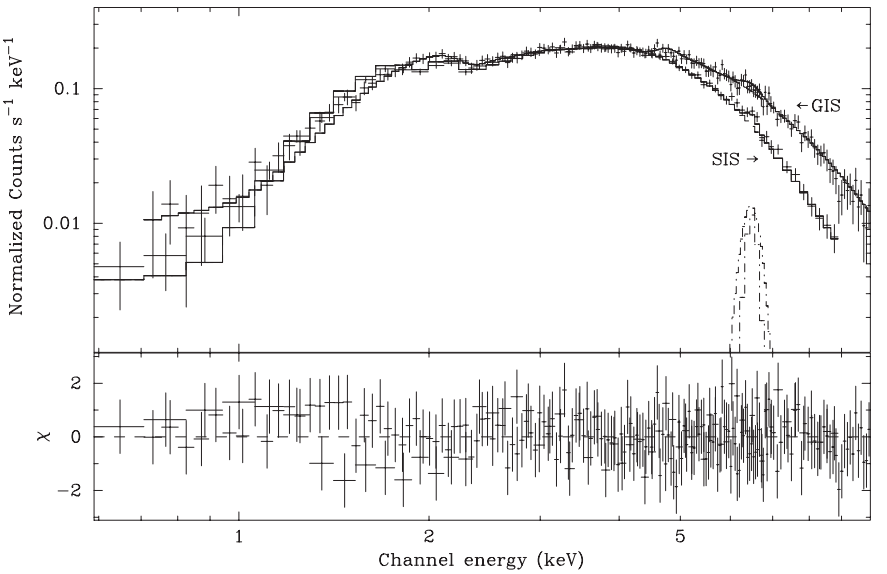

Figure 3. Same as in Fig. 2 but for the spectrum at low intensity level.

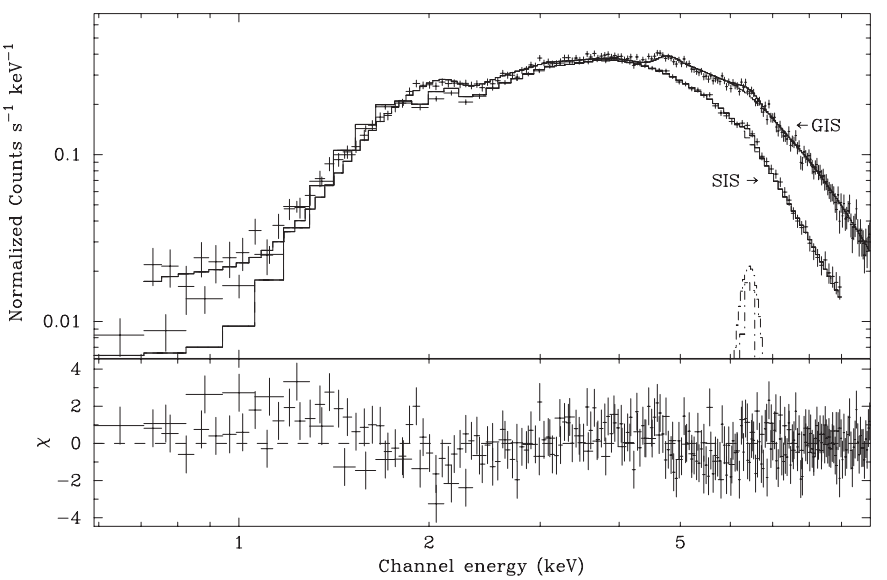

Figure 4. The spectrum measured during the entire observation is shown here with all other details same as in Fig. 2. Unlike the spectra in the low and high intensity levels (Figs. 2 and 3), the residuals show systematic differences between the data and the best fitted spectral model.

After fitting the high and low state spectra as above, we tried to fit the total spectrum (for the full time duration) with the same model. Though we obtained a reasonable reduced χ^2 of ~ 1.2, the parameters, except the line-centre energy, could not be constrained and the best fit model shows structured residuals between 1.0 and 3.0 keV (Fig. 4). In Table 1, we give the best fit model parameters with the 90% error estimates.

Table 1. The spectral parameters of the states with 90% error bars (N_H: Column density, PL norm: Power law normalization and $L_{2-10\ \mathrm{keV}}$: Unabsorbed luminosity in the 2–10 keV range).

Parameters	High	Low	Total
N_H (10^{22} cm^{-2})	$3.44^{+0.13}_{-0.12}$	$2.01^{+0.14}_{-0.18}$	2.81
Γ (Photon index)	$0.64^{+0.05}_{-0.05}$	$0.49^{+0.11}_{-0.15}$	0.62
PL norm (photons keV^{-1} cm^{-2} s^{-1})	$0.03^{+0.002}_{-0.002}$	$0.005^{+0.001}_{-0.001}$	0.013
Line energy (keV)	$6.38^{+0.03}_{-0.06}$	$6.49^{+0.08}_{-0.13}$	$6.43^{+0.07}_{-0.06}$
Line width (keV)	$0.006^{+0.11}_{-0.006}$	$0.013^{+0.24}_{-0.003}$	0.016
Line flux (10^{-4} photons cm^{-2} s^{-1})	$5.60^{+11.76}_{-1.55}$	$1.63^{+9.16}_{-0.70}$	2.07
Equivalent width (eV)	64.5	73.0	49.5
Cut-off energy (keV)	$6.47^{+0.38}_{-0.35}$	$4.41^{+0.37}_{-0.28}$	6.17
e-folding energy (keV)	$8.54^{+4.45}_{-1.65}$	$7.82^{+0.84}_{-1.04}$	7.83
Red. χ^2 (d.o.f.)	0.86 (260)	0.65 (219)	1.18 (260)
$L_{2-10\ \mathrm{keV}}$ (10^{36} ergs s^{-1})	3.65	0.80	1.71

For the composite spectrum, the model parameters are not constrained well and error estimates are not given. Continuum parameters are identical within error-bars while the line flux is lower by a factor of $\sim$4. The e-folding energy is not well constrained in the high state. This is possibly due to the limited energy range offered by ASCA. But in the low state, it is comparatively better constrained.

4. Discussion

The main objective of our work was to measure the spectral parameters of the pulsar 4U 0114 + 65 in its high and low states with the now known model components that fit the broad band spectrum well and to study the iron emission line parameters *vis-a-vis* the column density (N_H) and continuum parameters at different orbital phases and intensity levels. As enunciated in the results, the most suitable model describing the source in the different intensity states with ASCA was found to be a power law modified by a cut-off, along with an exponential absorption along the line of sight. The presence of a Gaussian line at $\sim$6.4 keV, the fluorescent iron line, was also confirmed in both the spectra. It can be seen that as the unabsorbed luminosity between the two states varies by a factor of $\sim$4.5, there is a little change in the spectral parameters of the continuum, i.e., in the photon index and the column density (N_H). The most significant difference between the high and low state spectra is a change in the iron-line flux by a factor similar to the change in the continuum.

It is pertinent to compare our results with those obtained from other satellites. In order to do that, we have projected in a nutshell in Table 2, the spectral parameters of this pulsar as measured with other satellites. We have also mentioned the orbital phases during which those observations were made to examine if there is any orbital phase dependence of the spectral parameters. The orbital period and the epoch was taken from Corbet *et al.* (1999). We have specifically mentioned the high and low states in the table to bring out any possible differences.

Table 2. The spectral parameters obtained from various satellites. The high and low states being designated as H and L respectively. (N_H: Column density, Γ: Power law index, E_c: Cut-off energy, E_f: e-folding energy, EW: Equivalent width of the 6.4 keV Fe line, L: Luminosity) and (ϕ: Orbital phase, S: Satellite, A: ASCA, B: BeppoSAX, I: Integral, R: RXTE, EX: EXOSAT, G: GINGA, EN: Einstein).

ϕ (S)	N_H (10^{22} cm^{-2})	Γ	E_c (keV)	E_f (keV)	EW (eV)	L (10^{36} ergs s^{-1})
0.19 (A)	$3.44^{+0.13}_{-0.12}$	$0.64^{+0.05}_{-0.05}$	$6.47^{+0.38}_{-0.35}$	$8.54^{+4.45}_{-1.65}$	64.5	3.65 (H)
	$2.01^{+0.14}_{-0.18}$	$0.49^{+0.11}_{-0.15}$	$4.41^{+0.37}_{-0.28}$	$7.82^{+0.84}_{-1.04}$	73.0	0.80 (L)
0.67 (B)	$9.7^{+0.7}_{-0.9}$	$1.33^{+0.09}_{-0.16}$	$12^{+2.0}_{-3.0}$	$21^{+4.0}_{-3.0}$	–	1.35 (H)
	$15.4^{+2.0}_{-1.7}$	$0.9^{+0.2}_{-0.2}$	$6.0^{+0.9}_{-0.7}$	$17^{+5.0}_{-3.0}$	80	0.37 (L)
0.85 (I)	–	$1.6^{+0.5}_{-0.5}$	$9.0^{+14.1}_{-8.8}$	$22.1^{+12.1}_{-6.0}$	–	1.8 (H)
0.82 (R)	$3.2^{+0.3}_{-0.3}$	$1.28^{+0.04}_{-0.05}$	$8.1^{+0.4}_{-0.4}$	$19.2^{+1.1}_{-1.0}$		1.25 (H)
	$4.1^{+0.4}_{-0.4}$	$1.63^{+0.04}_{-0.02}$	$11.3^{+0.8}_{-0.9}$	$22.4^{+6.7}_{-4.7}$	250	0.2 (L)
0.35 (EX)	$9.4^{+1.9}_{-1.9}$	$2.47^{+0.30}_{-0.30}$	–	–	526	0.45 (L)
0.36 (G)	$2.9^{+0.2}_{-0.2}$	$0.92^{+0.02}_{-0.02}$	$7.1^{+0.3}_{-0.3}$	$16.1^{+0.8}_{-0.8}$	70	5.0 (H)
	$4.7^{+0.6}_{-0.6}$	$1.07^{+0.03}_{-0.03}$	$6.8^{+1.0}_{-1.0}$	$15.4^{+4.0}_{-4.0}$	340	0.33 (L)
0.78 (EN)	$3.2^{+1.0}_{-1.0}$	$1.2^{+0.1}_{-0.1}$	–	–	–	2.11 (H)
	$3.2^{+1.0}_{-1.0}$	$1.2^{+0.3}_{-0.3}$	–	–	–	0.12 (L)

Note: The luminosities quoted in both the tables have been calculated with the distance to the pulsar as 7 kpc.

The RXTE and GINGA observations found marginal evidence for an increase of N_H during the low states while the BeppoSAX observations found N_H to increase by a factor of 2 in the low state. We note that in any of the three cases mentioned above, the increase in N_H by itself cannot explain occurrence of the low state. The galactic column density along the line of sight of 4U 0114 + 65 is $\sim 0.8 \times 10^{22}$ cm^{-2}. This is about an order of magnitude lower than the column density values of 4U 0114 + 65 obtained previously or in the present work. The N_H values measured with ASCA seem to compare well with that obtained with RXTE and GINGA, though the ASCA observation shows a slight decrease in the value of N_H in the low state, and the N_H values in the present work are a factor of $\sim$2–4 times lesser than that measured with BeppoSAX. From Table 2, if we compare only the high state observations or only the low state observations, we do not find any clear orbital phase dependence of the N_H or the equivalent width of the iron line. If the soft X-ray absorption is due to the material in the outflowing wind from the companion star and if the iron emission line is produced by the reprocessing of the continuum hard X-rays in this material, a smooth orbital phase dependence of the N_H and the equivalent width on orbital phase is expected. A similar finding in another pulsar GX 301–2 was interpreted in terms of a clumpy structure of the stellar wind (Mukherjee & Paul 2004).

Regarding photon index of the power law component, Table 2 shows that apart from the results from EXOSAT which point towards a very steep power law, the results from other satellites generally indicate a Γ of ~ 1. The unusually high value of Γ with

EXOSAT may be due to the slightly different spectral model used and the limited band width. The values of Γ obtained with ASCA is somewhat lower than 1. On the whole it is seen that Γ for this pulsar does not change appreciably with X-ray intensity.

From Table 2, we notice that the equivalent width of the fluorescent iron-line is comparatively higher in some of the low state observations and on most occasions (with BeppoSAX and RXTE), the 6.4 keV line is better detected in the low state. However with ASCA, we report the detection of the iron-line in both the states with appreciable and similar equivalent widths (Table 2). Since ASCA has the best spectral resolution in comparison to the other detectors mentioned herein, the measurements of the iron line parameters is likely to be most accurate with ASCA.

A hint of a soft excess was reported in the BeppoSAX spectra of this source by Masetti *et al.* (2005). They showed an apparent presence of the soft excess below 3 keV which they fitted with a $\sim$0.3 keV thermal component. However, in any of the ASCA fits covering an energy band lower compared to the reported BeppoSAX spectrum, we did not find any signature of the so-called soft excess as found in the spectra of many X-ray pulsars (Paul *et al.* 2002; Hickox *et al.* 2004). Moreover, in the case of 4U 0114 + 65, for the unabsorbed flux observed with ASCA in the high state ($\sim 6 \times 10^{-10}$ ergs cm^{-2} s^{-1}) along with the N_H of 3.4×10^{22} atoms cm^{-2} falls into the region in Fig. 1 of Hickox *et al.* (2004) which shows a collection of pulsars lacking soft excess.

During our observation, the transition of 4U 0114 + 650 between the high and the low state is abrupt. Similar abrupt flux changes have been observed in another pulsar GX 1 + 4 which also shows aperiodic transitions between its high and low states and thus requires special mention here. Naik *et al.* (2005) studied GX 1 + 4 for an extended period with observations by BeppoSAX and reported an order of magnitude decrease in the X-ray flux for a part of the observation, similar to the present observation of 4U 0114 + 650. In GX 1 + 4, the absorption column density was an order of magnitude higher in the low state, which is not the case for 4U 0114 + 650. In addition, Naik *et al.* (2005) found a strong increase in the iron line equivalent width in the low state which is also different from what we have observed in 4U 0114 + 650.

Equivalent width of the iron line is found to increase appreciably in the low states of several other pulsars like Her X-1 (Naik & Paul 2003), LMC X-4 (Naik & Paul 2004) and SMC X-1 (Vrtilek *et al.* 2005). The high and low states of the latter sources are part of the super-orbital period arising due to a precessing warped inner accretion disk. Though the pulsar 4U 0114 + 650 is reported to have a super-orbital period (Farrell *et al.* 2005), the abrupt decrease in X-ray flux over a few thousand second time scale reported here can not be assigned to the precession of a warped accretion disk. The change in luminosity during our observation can be ascribed to a local change in the density of the stellar wind from which the pulsar accretes material. The rise and fall times of 1–2 ks as can be seen in Fig. 1, and an assumed orbital velocity of a few hundred km per sec indicates clumpiness of the stellar wind at a length scale of about 10^{10-11} cm. The long term light curve of this source measured with the RXTE-ASM does not have enough sensitivity to measure incoherent intensity variations at the time scale of a few ks. During the ASCA observation, the iron line flux decreased with luminosity and has a direct correlation with the continuum luminosity (Table 1). It supports a picture in which the amount of fluorescence material, like in the form of a circumstellar shell at a large distance has remained unchanged but the local accretion has changed.

5. Conclusion

In this paper, we have reported an accurate measurement of the spectral parameters of the HMXB pulsars 4U 0114 + 650 in two different intensity levels. We have detected iron emission lines of similar equivalent width in both the intensity levels and the other spectral parameters are found to be similar in the two intensity levels. This shows that the intensity variations at a time scale of a few hours observed in 4U 0114 + 650 was not due to increased absorption, but possibly due to wind density that causes changes in the accretion rate. We have compared the present observation of this object with that done by other X-ray observatories and also with other HMXB pulsars which show widely different intensity states. 4U 0114 + 650 is found to have characteristics different from many other HMXB pulsars.

Acknowledgements

This research has made use of data obtained from the High Energy Astrophysics Science Archive Research Center (HEASARC), provided by NASA's Goddard Space Flight Center. We would also like to thank the ASCA team for providing the data in the archive. UM would like to acknowledge the Kanwal Rekhi Scholarship of TIFR Endowment Fund for partial financial support.

References

Apparao, K. M. V., Bisht, P., Singh, K. P. 1991, *ApJ*, **371**, 772.
Bonning, E. W., Falanga, M. 2005, *A&A*, **436**, L31.
Corbet, R. H. D., Finley, J. P., Peele, A. G. 1999, *ApJ*, **511**, 876.
Crampton, D., Hutchings, J. B., Cowley, A. P. 1985, *ApJ*, **299**, 839.
Dower, R., Kelley, R., Margon, B., Bradt, H. 1977, *IAUC*, **3144**, 2.
Ebisawa, K. 1997, *AAS*, **29**, 1388.
Farrell, S. A., Sood, R. K., O'Neill, P. M. 2005, *astro-ph/0502008*.
Finley, J. P., Belloni, T., Cassinelli, J. P. 1992, *A&A*, **262**, L25.
Hall, T. A., Finley, J. P., Corbet, R. H. D., Thomas, R. C. 2000, *ApJ*, **536**, 450.
Hickox, R. C., Narayan, R., Kallman, T. R. 2004, *ApJ*, **614**, 881.
Koenigsberger, F., Swank, J. H., Szymkowiak, A. E., White, N. E. 1983, *ApJ*, **268**, 782.
Masetti, N., Orlandini, M., Dal Fiume, D., Del Sordo, S., Amati, L., Frontera, F., Palazzi, E., Santangelo, A. 2006, *A&A*, **445**, 653.
Mukherjee, U., Paul, B. 2004, *A&A*, **427**, 567.
Naik, S., Paul, B. 2003, *A&A*, **401**, 265.
Naik, S., Paul, B. 2004, *ApJ*, **600**, 351.
Naik, S., Paul, B., Callanan, P. J. 2005, *ApJ*, **618**, 866.
Paul, B., Nagase, F., Endo, T. *et al.* 2002, *ApJ*, **579**, 411.
Reig, P., Chakrabarty, D., Coe, M. J., Fabregat, J., Negueruela, I., Prince, T. A., Roche, P., Steele, I. A. 1996, *A&A*, **311**, 879.
Shafer, R. A., Haberl, F., Arnaud, K. A. 1989, XSPEC: An X-ray Spectral Fitting Package, ESA TM-09 (Paris:ESA).
Tanaka, Y., Inoue, H., Holt, S. S. 1994, *PASJ*, **46**, L37.
Vrtilek, S. D., Raymond, J. C., Boroson, B., McCray, R. 2005, *ApJ*, **626**, 307.
Yamauchi, S., Asaoka, I., Kawada, M., Koyama, K., Tawara, Y. 1990, *PASJ*, **42**, L53.
Yokogawa, J., Paul, B., Ozaki, M. *et al.* 2000, *ApJ*, **539**, 191.